DECISION FUSION OF SYMMETRICALLY TRAINED CNN CLASSIFIERS FOR DIAGNOSIS OF CHEST CT IMAGES

Gabriela-Loredana GHENEA[1], Victor-Emil NEAGOE[2]

This paper is dedicated to decision fusion of an ensemble of M symmetrically trained Convolutional Neural Network (CNN) classifiers with identical architectures for chest CT image diagnosis corresponding to K classes. There are considered two decision fusion algorithms: Dempster Fusion theory versus net maximization. The experiments use Covid-19&Normal&Pneumonia_CT_image Kaggle dataset. This choice corresponds to decision fusion algorithm implementation for K=3 classes and M = [2, 3, 4, 5, 6, 7] CNN classifier modules. The advantage of the proposed decision fusion method as reference to a standalone classifier is obvious, leading to an average accuracy improvement of about 2.70%. Regarding the comparison of the two decision fusion algorithms, the D-S method obtains a slightly better accuracy than the net maximization.

Keywords: convolutional neural networks (CNNs), decision fusion, Dempster-Shafer theory, net maximization, chest CT image classification, pneumonia and COVID-19 diagnosis.

1. Introduction

The global COVID-19 pandemic came with a need for rapid and accurate diagnostic tools. Therefore, the use of convolutional neural networks (CNNs) for classifying chest CT images has shown significant promise. This paper explores an innovative approach that takes advantage of the power of M CNN architectures, combining their strengths to enhance the accuracy of chest CT images diagnosis, distinguishing between COVID-19, pneumonia and normal cases.

Currently, research in this field provides numerous studies demonstrating the effectiveness of CNNs in medical image analysis. Recent work has focused on optimizing network architectures, improving data preprocessing techniques, and integrating a metric-based approach to refine diagnostic capabilities [1][2][3]. Despite these advancements, challenges such as overfitting and data generalization remain the subject of future research.

[1] Ph.D. Student., Faculty of Electronics, Telecommunications and Information Technology, National University of Sciences and Technologies POLITEHNICA Bucharest, Romania, e-mail: loredana.ghenea96@gmail.com

[2] Prof., Faculty of Electronics, Telecommunications and Information Technology, National University of Sciences and Technologies POLITEHNICA Bucharest, Romania, e-mail: victoremil@gmail.com

The purpose of this paper is to address these challenges by proposing a fusion model between the outputs of M classifiers that can distinguish between K classes by applying either Dempster-Shafer theory or Net-Maximization techniques. This fusion aims to exploit the strengths of each network, thereby improving diagnostic accuracy and robustness. Previous papers have addressed this area of study [4][5][6][7], providing a foundation for this research. While these studies are a solid base, this paper introduces several innovations. First, we employ multiple classifiers, joining their performances to improve the overall results. Additionally, this research is focusing on a multiclass classification, while previous studies depicted intelligent systems capable of COVID diagnosis (two-class classification).

By providing a review of the used methodologies and presenting experimental results, this paper contributes to the ongoing efforts to enhance automated classification of chest CT images.

2. Proposed architecture

The proposed architecture for diagnosis of chest CT images uses multiple concurrent CNN classifiers. For these experiments, we have chosen M = [2, 3, 4, 5, 6, 7] classifiers based on the VGG16 architecture [8]. The VGG model is known for its effectiveness in image classification tasks and consists of thirteen convolutional layers, three fully connected layers, followed by a SoftMax layer for output. The secret of this architecture is represented by the combination between convolutional layers which use receptive fields of 3x3 for feature extraction and max-pooling layers to reduce the dimensions.

For the proposed system, we have chosen M modules with identical architecture and identical training strategy. Each of the VGG classifiers has been trained to classify images into three categories: COVID-19, pneumonia and normal. Each classifier was trained with an identical number of images from each class to ensure symmetrical learning. The A100 GPU has been used for calculations provided by the Google Colab cloud GPU provider. Training parameters include a 64-batch size, 50 epochs, and Adam as the optimizer with a 0.0001 learning rate. After several tests, we have reached the conclusion that these settings were the best choice. Once trained, the outputs from these classifiers are fed into the decision fusion system. The decision fusion process combines the individual predictions to improve the overall classification accuracy. We employ two decision fusion techniques: Dempster-Shafer Theory (D-S Theory) [9] and Net Maximization Theory. A block diagram of the presented architecture is depicted in Fig. 1.

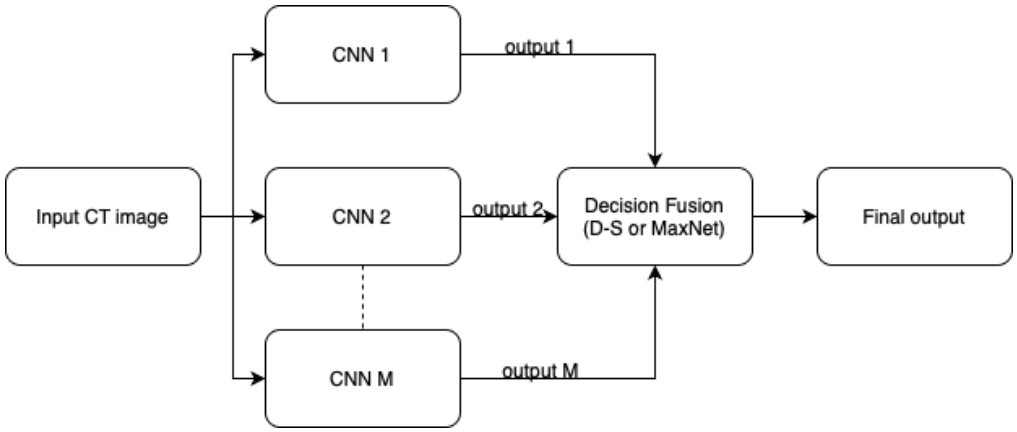

Fig. 1. Block diagram of proposed architecture

In the following sections, we will further present and detail the database, each decision fusion algorithm and highlight experimental results.

3. Dempster-Shafer theory for decision fusion of CNN classifiers

As presented in chapter 2, the proposed system uses M different CNN classifiers and combines their outputs to provide a final decision. One of the algorithms used for the decision fusion is the Dempster-Shafer theory.

Prior research has demonstrated that this theory of evidence is a good candidate for computing the belief in uncertain cases [5][7][10][11]. We will further present the general equations for this algorithm, for K classes and M classifiers. For this application we have used K = 3 classes (COVID, Pneumonia and Normal) and M = [2, 3, 4, 5, 6, 7] classifiers.

Considering z as the input image fed to the system, we compute the evidence belief for class k and classifier n (1):

$$m_k^{(n)} = \frac{1}{1+ e^{-net_k^{(n)}(z)}} \tag{1}$$

After computing the evidence of belief for each class, we apply the Dempster-Shafer theory to deduce (2):

$$m_k(z) = \frac{\prod_{n=1}^{M} m_k^{(n)}(z)}{\sum_{h=1}^{k}(\prod_{n=1}^{M} m_k^{(n)}(z))} \tag{2}$$

Image z will be classified as class j according to the following relation (3)

$$m_j(z) = MAX\{m_k(z)\} \tag{3}$$

4. Net maximization theory

To explore multiple decision fusion algorithms, we have chosen to combine the outputs of the three modules using two different methods. Net maximization theory is a simple, but powerful technique that can improve classification accuracy significantly. This method has proven to be a strong technique for decision fusion between two classifiers on X-Ray and CT images classified in two classes [4][6]. In this paper the theory has been extended to a decision fusion between M classifiers used for multi-class diagnosis.

Net-Maximization theory aims to compute a final decision based on the net function for each CNN classifier.

Considering z = the input image and M = number of classifiers, it will be classified as class j according to the following relation (4):

$$m_j(z) = MAX\{net_{1,}\, net_2, \dots, net_M\} \tag{4}$$

In the equation above, net_i is the net output for CNN_i, where i=1,..M. The output of a CNN represents the weighted sum of the input values.

5. Database

Within this paper we have used the "COVID-19, Normal, and Pneumonia Chest CT Images" dataset [12]. This is a public resource that is available online on Kaggle website. It provides CT images classified into three categories: 2035 COVID-19 scans, 3390 pneumonia scans and 2119 normal scans. To increase the diversity of the images, the data for each class has been increased by 50% by performing a simple data augmentation technique consisting in random horizontal and vertical flips and random rotation with 0.2. After this key step has been applied, we made sure that the dataset is balanced, having an equal number of images from each class. To accomplish this, after the data augmentation has been performed, some images were removed from the classes that had more images than the smallest class (COVID-19). This has resulted in 3052 images from each class.

One important challenge when dealing with medical image classification is the data availability. To highlight the efficiency of our classification system, we have chosen to use a smaller subset of images and diminish the database up to 40 times (3052 / 40 = 76 images per class) from which 75% (76 * 0.75 = 57 images per class) were used as training data and 25 % (76 * 0.25 = 19 images per class) were used as validation data in the training process.

For this experiment, we have chosen to diminish the database to [4, 5, 6, 8, 10,12, 16, 20, 40] times, resulting in the following number of training images per class for each experiment: 572, 457, 381, 286, 228, 190, 143, 114, 57.

For all experiments that were mentioned above, the number of test images per class is 500. Fig. 2, Fig. 3, and Fig. 4 depict some examples of images from the database.

Fig. 2. COVID CT image

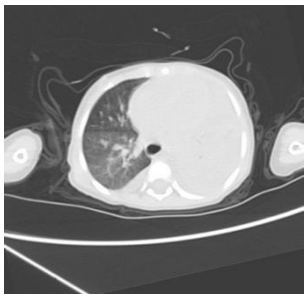

Fig. 3. Pneumonia CT image

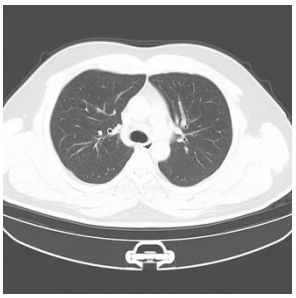

Fig. 4. Normal CT image

6. Experimental results

This section will depict a comprehensive analysis of the experimental results. To present the performance of the system, we have computed the overall accuracy (OA), using True Positives (TP), True Negatives (TN), False Positives (FP) and False Negatives (FN).

$$OA = 100 \times \frac{TP+TN}{TP+TN+FP+FN} \tag{5}$$

In tables 1-6 we have presented the detailed results for each experiment. For each case we have also computed the percent of improvement after decision fusion with respect to the average results of individual CNN modules.

Tables 1 and 2 present the experimental results for two different setups: Table 1 with M = 2 classifiers and Table 2 with M = 3 classifiers. Setup presented in Table 1 uses two classifiers (CNN1 and CNN2). The accuracy for Max-Net (OA MAX) and D-S accuracy (OA D-S) are consistently higher than the individual classifiers' OAs. The D-S method shows improvement over Max-Net in all cases, with the highest improvement (5.914%) observed for 57 test images per class.

The system from Table 2 uses three classifiers (CNN1, CNN2, CNN3). Like Table 1, the OA MAX and OA D-S values are higher than individual classifier accuracies. The D-S combination method also shows an improvement over OA MAX, with the highest improvement (8.135%) observed for 57 test images per class.

The results in both tables suggest that the Dempster-Shafer (D-S) combination method is effective in improving overall accuracy compared to individual classifiers and Max-Net fusion method (OA MAX). The improvements are more pronounced in scenarios with fewer train images per class, and the

improvement is greater when using three classifiers compared to two. This indicates that increasing the number of classifiers in an ensemble setup may lead to better classification performance and more robust results, especially when the dataset size is small.

Table 1

Experimental results for M = 2 classifiers

Train images per class	Test images per class	OA CNN1 [%]	OA CNN2 [%]	OA MAX [%]	OA D-S [%]	Average D-S improvement [%]
572	500	95.46	96.33	97.66	97.73	1.914
457	500	94.6	94.06	96.53	96.74	2.555
381	500	93.8	94.6	96.4	96.88	2.845
286	500	94.06	94.13	96.2	96.66	2.726
228	500	91.86	92.13	94.4	94.53	2.756
190	500	90.53	88.26	93.33	93.34	4.413
143	500	89.8	90.06	92.53	92.66	3.036
114	500	89	88.26	90.93	91.13	2.821
57	500	81.6	78.53	84.66	84.8	5.914

Table 2

Experimental results for M = 3 classifiers

Train images per class	Test images per class	OA CNN1 [%]	OA CNN2 [%]	OA CNN3 [%]	OA MAX [%]	OA D-S [%]	Average D-S improvement [%]
572	500	95.66	95.86	96.06	96.73	97.86	1.98
457	500	95.06	94.53	95	96.4	97.26	2.633
381	500	95.13	90.73	95.2	96.73	96.8	4.125
286	500	94.6	92.8	93.33	95.26	95.8	2.939
228	500	91.8	92	93.26	95.06	95.86	3.487
190	500	91.13	91.33	92.13	93.8	94.86	3.412
143	500	89.2	89.8	90.26	92.06	93.2	3.521
114	500	88.66	89.4	90.66	91.73	91.93	2.11
57	500	80.93	82.06	83.4	87.46	89.46	8.135

Tables 3 and 4 present experimental results for M = 4 and 5 classifiers. In both tables, the accuracy (OA) decreases as the number of training images per class decreases, which is expected due to reduced training data. However, the D-S (Dempster-Shafer) combination method consistently outperforms individual classifiers (CNN1 through CNN4 or CNN5) and the Max-Net fusion method, demonstrating an improved accuracy, especially as the training set size reduces. This statement is sustained by Table 3 (M = 4 classifiers) with a maximum improvement of 9.1% when the training images per class drop to 57. Table 4 (M =

5 classifiers) further supports this trend, with even better results for D-S, achieving a maximum improvement of 6.231% for the smallest dataset (57 images per class).

Table 3

Experimental results for M = 4 classifiers

Train images per class	Test images per class	OA CNN1 [%]	OA CNN2 [%]	OA CNN3 [%]	OA CNN4 [%]	OA MAX [%]	OA D-S [%]	Average D-S improvement [%]
572	500	95.66	95.86	96.06	96	97.13	98.13	2.187
457	500	93.6	93.6	95.95	94.13	96.93	97.13	2.199
381	500	93.33	94.2	92.66	92.73	96.2	96.86	4.493
286	500	93.93	92.2	92.8	93.6	95.26	96	3.004
228	500	94	93.26	92.26	92.93	95.73	96.26	3.958
190	500	89.93	90.73	90.8	89.8	93.93	94.4	4.54
143	500	90.2	89.2	89.66	88.86	93.4	93.53	4.784
114	500	88.2	87.73	86.2	87.93	90.73	91.4	4.979
57	500	78.26	80.8	80.86	82.66	86.4	89.2	9.1

Table 4

Experimental results for M = 5 classifiers

Train images per class	Test images per class	OA [%]							Average D-S improvement [%]
		CNN 1	CNN 2	CNN 3	CNN 4	CNN 5	MAX	D-S	
572	500	96.73	96.46	96.2	97.06	95.93	98.33	98.86	2.451
457	500	94.86	94.8	94.86	94.93	94.4	96.93	97.86	3.375
381	500	94.73	94.53	93.46	94.6	94.53	95.93	97	2.575
286	500	92.93	92.4	94.2	93.93	92.93	95.4	96.13	2.89
228	500	91.33	91.8	91.8	92.26	91.53	94.8	95.53	3.956
190	500	91.73	89.66	90.53	91.26	91.13	94	94.93	4.096
143	500	88.66	88.33	89.93	89.8	90.26	92.8	93.73	4.11
114	500	87.6	89.06	85.73	88.93	85.4	91.73	92.2	5.776
57	500	83.2	80.33	81.53	82.26	84.66	88.33	88.66	6.231

Tables 5 and 6 show the experimental results with M = 6 and M = 7 classifiers, respectively. The trend in both tables continues to confirm that combining multiple classifiers, particularly using the D-S (Dempster-Shafer) method, leads to higher overall accuracy (OA), especially as the number of training images per class decreases.

In Table 5 (M = 6 classifiers) the D-S approach shows an increasing percentage of improvement as the training set size decreases, peaking at 9.078% improvement for the smallest dataset (57 images per class). Table 6 (M = 7

classifiers) further emphasizes the benefits of using more classifiers, with the D-S method achieving even higher improvement rates, reaching up to 10.85% for 57 training images per class. These results highlight the scalability and efficacy of the D-S combination in multi-classifier ensembles.

Table 5

Experimental results for M = 6 classifiers

Train images per class	Test images per class	OA [%]								Average D-S improvement [%]
		CNN 1	CNN 2	CNN 3	CNN 4	CNN 5	CNN 6	MAX	D-S	
572	500	96.93	96.33	96.53	95.66	96.2	96.6	98.06	98.8	2.49
457	500	94.26	95.6	94.8	95.46	95.8	94.93	96.93	97.6	2.344
381	500	94.66	94.4	94.46	95.26	95	92.53	96.4	97.33	3.802
286	500	93.46	92.46	92.26	92.13	93.53	92.73	95.46	96.2	3.296
228	500	89	90.73	91.33	91.53	91.26	91.2	93.93	95.2	4.352
190	500	89.86	89.6	90.73	91.13	89.6	91.66	93.33	94.93	4.745
143	500	89.53	88.86	89	89.2	88.66	88.4	93.86	94.26	6.472
114	500	88.13	87.73	88	86.2	86.6	88.86	92.2	92.53	5.471
57	500	84.33	79.4	83.6	81.46	82.06	81.86	87.93	89.4	9.078

Table 6

Experimental results for M = 7 classifiers

Train images per class	Test images per class	OA [%]									Average D-S improvement [%]
		CNN 1	CNN 2	CNN 3	CNN 4	CNN 5	CNN 6	CNN 7	MAX	D-S	
572	500	96.8	96.33	96.86	96	92.4	96.53	95.73	97.66	98.46	2.424
457	500	95.73	95.46	94.8	95.93	95.33	96.06	95.8	97.4	97.6	1.741
381	500	94.93	94.8	94.73	94.26	94.06	95.93	95.53	96.8	97.26	1.598
286	500	92.73	94.06	93.2	92.66	93.93	94.33	93.8	95.66	96.66	2.759
228	500	91.73	92.33	91.46	91.13	92.2	91.93	90.66	94.33	95.73	4.858
190	500	88.66	91.33	90.86	90.86	89.6	90.6	90.2	94.06	95.66	5.819
143	500	88.66	87.53	91.26	90.06	90.13	87.73	89.06	93.06	93.66	5.956
114	500	88.13	86.66	88.33	89.26	87.33	87.53	89.6	92.06	93.8	5.911
57	500	82.26	81.4	85.33	86.4	80.4	84.46	81.4	89.8	91.93	10.85

Table 7 and the corresponding graph (Fig. 5) present the maximum overall accuracy (OA) achieved by three methods — MAX, D-S, and single module — as the number of CNN modules (M) increases from 2 to 7. Dempster-Shafer

method consistently provides the highest accuracy across all values of M. The accuracy reaches its peak at M = 5 with an OA of 98.86% before slightly decreasing at M = 6 and M = 7, still maintaining the highest performance across methods. Max-Net method performs second best, with its peak accuracy of 98.33% at M = 5. It fluctuates slightly for different values of M but remains lower than D-S. The graph visually confirms this trend, with D-S consistently leading, followed by MAX, while the individual module accuracy remains lower.

Table 7

Experimental results – maximum accuracy for each M value

M	OA MAX	OA DS	OA per module
2	97.66	97.73	96.33
3	96.73	97.86	96.06
4	97.13	98.13	96.06
5	98.33	98.86	97.06
6	98.06	98.8	96.93
7	97.66	98.46	96.86

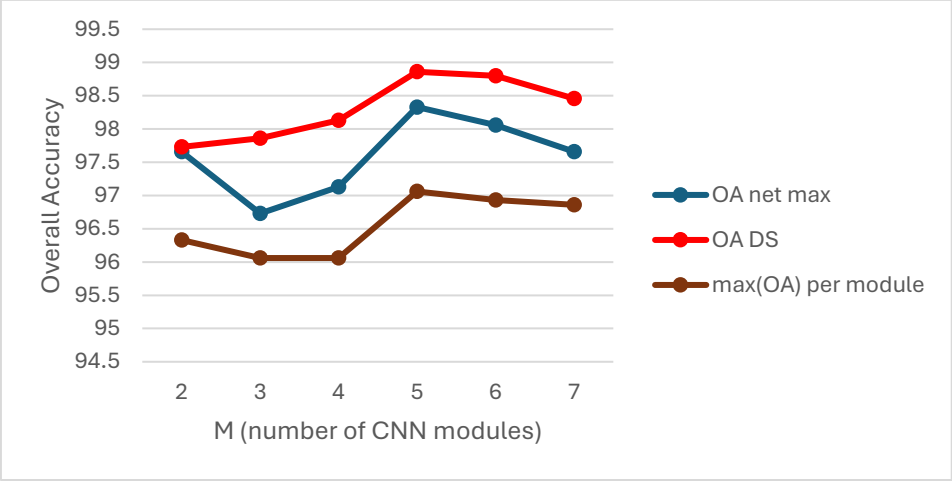

Fig. 5. Overall Accuracy as a function of number of CNN modules

In the next graph (Fig. 6) we have highlighted the results for M = 5 classifiers, combination for which we have obtained the best performance. We can observe that the D-S method consistently performs the best across most of the range, followed by the Max-Net method. It highlights the conclusion that Dempster-Shafer is the most robust method to the reduction in training data.

Fig. 6. Overall Accuracy as a function of number of train images for M = 5 classifiers

Some other important parameters when classifying medical images are specificity, sensitivity, miss alarm rate (MAR) and false alarm rate (FAR). There parameters were computed for the optimum case with M = 5 and the results are depicted in table 8. To compute these parameters, we have considered two classes: sick (comprised of COVID and Pneumonia samples) and healthy (Normal samples).

Table 8

Experimental results – specificity, sensitivity, MAR and FAR for M = 5

	Nr img	572	457	381	286	228	190	143	114	57
CNN1	**Sensitivity**	0.659	0.660	0.655	0.661	0.664	0.658	0.657	0.645	0.617
	Specificity	0.990	0.970	0.970	0.954	0.914	0.928	0.880	0.920	0.932
	MAR	0.044	0.059	0.079	0.071	0.095	0.107	0.157	0.165	0.250
	FAR	0.010	0.030	0.030	0.046	0.086	0.072	0.120	0.080	0.068
	OA	96.73	94.86	94.73	92.93	91.33	91.73	88.66	87.6	83.2
CNN2	**Sensitivity**	0.661	0.657	0.651	0.645	0.651	0.646	0.653	0.624	0.635
	Specificity	0.982	0.984	0.976	0.972	0.970	0.970	0.910	0.938	0.840
	MAR	0.044	0.059	0.090	0.118	0.096	0.116	0.143	0.222	0.270
	FAR	0.018	0.016	0.024	0.028	0.030	0.030	0.090	0.062	0.160
	OA	96.46	94.8	94.53	92.4	91.8	89.66	88.33	89.06	80.33
CNN3	**Sensitivity**	0.660	0.660	0.655	0.655	0.662	0.655	0.649	0.649	0.619
	Specificity	0.982	0.964	0.966	0.958	0.932	0.940	0.946	0.938	0.914
	MAR	0.048	0.063	0.081	0.089	0.088	0.107	0.126	0.134	0.258
	FAR	0.018	0.036	0.034	0.042	0.068	0.060	0.054	0.062	0.086
	OA	96.2	94.86	93.46	94.2	91.8	90.53	89.93	85.73	81.53
CNN4	**Sensitivity**	0.662	0.656	0.657	0.664	0.658	0.660	0.642	0.621	0.635
	Specificity	0.984	0.986	0.974	0.890	0.950	0.946	0.964	0.986	0.910
	MAR	0.036	0.058	0.068	0.121	0.086	0.082	0.135	0.193	0.207
	FAR	0.016	0.014	0.026	0.110	0.050	0.054	0.036	0.014	0.090
	OA	97.06	94.93	94.6	93.93	92.26	91.26	89.8	88.93	82.26
CNN5	**Sensitivity**	0.660	0.659	0.661	0.657	0.652	0.665	0.652	0.629	0.643
	Specificity	0.978	0.974	0.964	0.956	0.948	0.900	0.940	0.974	0.886
	MAR	0.050	0.058	0.060	0.083	0.111	0.105	0.118	0.173	0.203
	FAR	0.022	0.026	0.036	0.044	0.052	0.100	0.060	0.026	0.114
	OA	95.93	94.4	94.53	92.93	91.53	91.13	90.26	85.4	84.66
MAX	**Sensitivity**	0.664	0.663	0.660	0.661	0.660	0.661	0.658	0.645	0.650

	Specificity	0.990	0.990	0.984	0.978	0.982	0.968	0.964	0.982	0.916
	MAR	0.020	0.024	0.044	0.048	0.046	0.056	0.074	0.108	0.150
	FAR	0.010	0.010	0.016	0.022	0.018	0.032	0.036	0.018	0.084
	OA	98.33	96.93	95.93	95.4	94.8	94	92.8	91.73	88.33
DS	**Sensitivity**	0.663	0.661	0.660	0.659	0.660	0.663	0.654	0.633	0.638
	Specificity	0.988	0.990	0.974	0.964	0.966	0.954	0.960	0.988	0.934
	MAR	0.026	0.033	0.053	0.069	0.061	0.061	0.093	0.147	0.177
	FAR	0.012	0.010	0.026	0.036	0.034	0.046	0.040	0.012	0.066
	OA	98.86	97.86	97	96.13	95.53	94.93	93.73	92.2	88.66

7. Conclusions

In this paper, we have explored the decision fusion of an ensemble of M symmetrically trained CNN classifiers with identical architectures for chest CT image diagnosis corresponding to three classes: COVID-19, pneumonia and normal. By implementing two decision fusion algorithms, Dempster-Shafer theory and net maximization, we have demonstrated the effectiveness of combining multiple CNN classifiers. Using a public dataset, our experiments showed that the proposed decision fusion method improved the average accuracy by approximately 2.70% compared to a standalone classifier. Furthermore, the Dempster-Shafer method achieved slightly better accuracy than the net maximization approach.

Comparing to existing classification systems using the same dataset, we have managed to improve the performance by using this decision fusion system. In [13] Asif et al. have used the same dataset with a customized convolutional neural network. Their architecture used the entire dataset for the training, 80% as training data (6035 images) and 20% as testing data (1509 images) The same database was used in [14] where Rani and Bharadwaj have used the same database with a custom architecture called Deep CT-NET. Results in [14] are based on a big database, since they have merged five databases to improve the accuracy of classification. Our system has obtained a higher performance than both references even if it has been trained on a diminished dataset (572 per class for training). Compared to the other two papers, this makes the architecture even more performant.

Future work will involve conducting more experiments with different types of classifiers to validate and extend the robustness of the decision fusion approach. Additionally, we plan to explore the performance of asymmetrically trained classifiers and while varying the number of CNN modules. These efforts aim to refine the decision fusion method, enhancing its applicability and accuracy in automated chest CT image diagnosis. Another potential improvement involves applying Generative Adversarial Networks (GANs) for data augmentation, which could enhance the diversity and volume of the dataset, leading to further improvements in classification performance.

REFERENCES

[1]. *Shi C, Shao Y, Shan F, Shen J, Huang X, Chen C, Lu Y, Zhan Y, Shi N, Wu J, Wang K, Gao Y, Shi Y, Song F.*, Development and validation of a deep learning model for multicategory pneumonia classification on chest computed tomography: a multicenter and multireader study, Quant Imaging Med Surg. 2023 Dec 1;13(12):8641-8656

[2]. *E. J. Mortani Barbosa Jr, B. Georgescu, S. Chaganti, G. B. Aleman, J. Broncano Cabrero, G. Chabin, T. Flohr, P. Grenier, S. Grbic, N. Gupta, F. Mellot, S. Nicolaou, T. Re, P. Sanelli, A. W. Sauter, Y. Yoo, V. Ziebandt, D. Comaniciu*, Machine learning automatically detects COVID-19 using chest CTs in a large multicenter cohort, European Radiology, vol. 31, pp. 8775-8785, May 2021, Springer

[3]. *Luo, Ju & Sun, Yuhao & Chi, Jingshu & Liao, Xin & Xu, Canxia*, A novel deep learning-based method for COVID-19 pneumonia detection from CT images. BMC Medical Informatics and Decision Making. (2022). 22. 10.1186/s12911-022-02022-1.

[4]. *L. G. Ghenea, V. E. Neagoe*, Concurrent convolutional neural networks with decision fusion to diagnose COVID-19 using chest Xray imagery, Proc. 13 th International Conference on Electronics, Computers, and Artificial Intelligence (ECAI), July 1-3, 2021, Pitesti, Romania,

[5]. *V. -E. Neagoe, G. -L. Ghenea*, An Approach of Dempster-Shafer Decision Fusion to Diagnose COVID-19 in Chest X-ray Imagery by Using Controlled Asymmetric Training of the two CNNs Ensemble, 2022 14th International Conference on Electronics, Computers and Artificial Intelligence (ECAI), Ploiesti, Romania, 2022, pp. 1-6.

[6]. *G. -L. Ghenea, V. -E. Neagoe*, Classification of Chest CT Images for COVID-19 Detection Using an Ensemble of Twin CNNs with Decision Fusion, 2023 15th International Conference on Electronics, Computers and Artificial Intelligence (ECAI), Bucharest, Romania, 2023

[7]. *G.-L. Ghenea, V.-E. Neagoe*, Decision Fusion of Two Asymmetric Trained CNN Classifiers to Detect COVID-19 in Chest X-ray Imaging: Dempster-Shafer versus Net Maximization, 1st Doctoral Symposium on Electronics, Telecommunications and Information Technology, October 2023, Bucharest, Romania

[8]. *K. Simonyan, A. Zisserman*, Very deep convolutional networks for large-scale image recognition, 'Proc. International Conference on Learning Representation (ICLR-2015), May 7-9, 2015, San Diego, California, USA, pp. 1-14.

[9]. *G. Shafer*, A Mathematical Theory of Evidence, vol. 42. Princeton, NJ, USA: Princeton Univ. Press, 1976.

[10]. *V. E. Neagoe, A. Ropot, and A. Mugioiu*, Real time face recognition using decision fusion of neural classifiers in the visible and thermal infrared spectrum, Proc. of the 2007 IEEE International Conference on Advanced Video and Signal based Surveillance (AVSS 2007), London (United Kingdom), 5-7 September 2007, pp.1-6.

[11]. *V. E. Neagoe, P. Diaconescu*, An ensemble of deep convolutional neural networks for drunkenness detection using thermal infrared facial imagery, Proc. 13th International Conference on Communications, June 18-20, 2020, Bucharest, Romania, pp 147-150.

[12]. COVID-19&Normal&Pneumonia_CT_Images, Kaggle, Available online: https://www.kaggle.com/datasets/anaselmasry/covid19normalpneumonia-ct-images

[13]. *S. Asif, Y. Wenhui, S. Jinhai, Z. Waheed, Y. Yueyang and H. Jin*, CVD19-Net: An Automated Deep Learning Model for COVID-19 Screening using Chest CT Images, 2022 IEEE International Conference on Bioinformatics and Biomedicine (BIBM), Las Vegas, NV, USA, 2022, pp. 2049-2058

[14]. *N. S. Rani and S. R. Bharadwaj*, Towards Understanding the COVID-19 Specific Patterns in Lung CT Scan Images using Deep CTNET Framework, 2022 International Conference on Futuristic Technologies (INCOFT), Belgaum, India, 2022, pp. 1-7